RZ 3218 (# 93264) 03/20/00
Physical Sciences 6 pages

Research Report

Measuring viscous dissipative interactions in dynamic force microscopy

U. Dürig

IBM Research
Zurich Research Laboratory
8803 Rüschlikon
Switzerland

Measuring viscous dissipative interactions in dynamic force microscopy

U. Dürig

IBM Research, Zurich Research Laboratory, 8803 Rüschlikon, Switzerland

Abstract

The periodic motion of a harmonic pendulum in an arbitrary force field including viscous damping is studied as it pertains to dynamic force microscopy. It is shown that the damping constant as a function of tip-sample distance and thus the dissipative force can be obtained unambiguously by measuring the driving-force amplitude versus displacement of the force sensor. This methodology provides the basis for quantitative force spectroscopy of dissipative interactions.

Interaction sensing in dynamic force microscopy essentially involves two fundamentally different physical mechanisms, namely conservative forces, which give rise to a shift of the resonance frequency, and dissipative interactions, which determine the amount of driving force that must be supplied in order to sustain a stationary oscillatory motion of the force sensor. To date, most of the published work is based on exploiting conservative forces for imaging purposes by means of noncontact dynamic force microscopy, a technique that was pioneered in the mid-nineties[1, 2, 3]. Dissipative interactions, on the other hand, have so far been only rarely discussed in the literature, although they constitute an important complementary observable[3, 4, 5]. In particular, a comprehensive theory that would allow one to relate in a quantitative manner experimental observables such as the amplitude of the driving force to physical quantities such as the dissipative tip-sample force is lacking. This Letter takes a step towards a quantitative understanding of dissipative force sensing. Using a first-order perturbative approach, a well-defined methodology is presented that allows one to extract the damping coefficient associated with a viscous dissipative interaction from experimentally measured power-loss characteristics.

We consider a dynamic force microscopy experiment in which the force sensor oscillates at the resonance frequency with a constant amplitude a_1 (see Fig. 1). The motion of the tip, termed orbital $\psi(t)$, is a periodic function, meaning that an appropriate driving force $F_0(t)$ is applied, which compensates for the energy loss due to dissipative interactions. The tip-sample force $F_{\mathrm{TS}} = F_{\mathrm{int}} + F_{\mathrm{diss}}$ can be decomposed into a conservative force $F_{\mathrm{int}}(x)$, which is an explicit function of the tip-sample distance x, and a dissipative force F_{diss}, which is antisymmetric with respect to inversion of the tip motion,[5] viz. the dissipative force at some position x during approach changes sign during retraction (note that F_{int} is even with respect to path inversion). In this Letter we assume that the dissipation originates from a viscous force $F_{\mathrm{diss}} = -\dot{\psi}\Gamma(x)$ that is proportional to the local tip velocity and a damping coefficient. For a harmonic orbital the velocity is an odd function with respect to path inversion. Hence, it follows that the damping coefficient $\Gamma(x)$ is an explicit function of the tip-sample distance alone. Note, however, that other types of dissipative interactions exist that cannot be mapped onto this framework. A prominent example as discussed in Ref. [5] is the well-known adhesion hysteresis, which is associated with mechanical instabilities in the tip-sample contact zone and which persists in the adiabatic limit, viz. for arbitrarily slow motion.

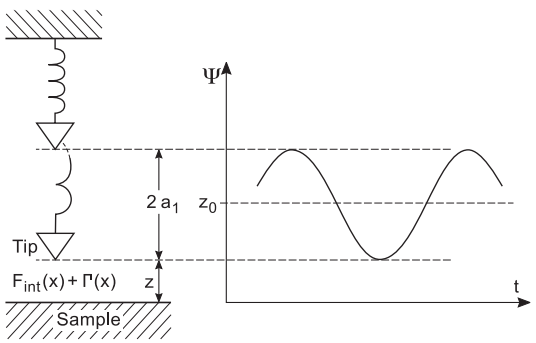

Figure 1: Schematic drawing of dynamic force sensing: z_0: offset parameter, a_1 amplitude of oscillation, $z = z_0 - a_1$: distance of closest approach. The tip-sample interaction comprises a conservative interaction $F_{\mathrm{int}}(x)$ and a dissipative viscous interaction, which is represented by a damping coefficient $\Gamma(x)$.

Let the force sensor be a one-dimensional harmonic oscillator with spring constant C and resonance frequency ω_0. The corresponding equation of motion for the tip orbital is

$$\frac{C}{\omega_0^2}\ddot{\psi}(t) + \dot{\psi}(t)\Gamma(z_0 + \psi(t)) + C\psi(t) - F_{\rm int}(z_0 + \psi(t)) = F_0(t), \tag{1}$$

where z_0 is an offset parameter that fixes the position of the force sensor with respect to the sample.

It is presumed that the tip-sample interaction is weak in the sense that the orbital deviates only slightly from a harmonic motion. This allows us to use a first-order perturbative approach, whereby the orbital function, is approximated by the lowest-order harmonic term $\psi(t) = a_1 \cos(\omega t)$. A refined analysis including higher harmonics and their implications for force sensing will be published elsewhere[5]. For the sake of simplicity we further assume a harmonic driving force $F_0(t) = F_0 \left[\cos\Theta \cos(\omega t) + \sin\Theta \sin(\omega t)\right]$, where Θ denotes the phase angle between the tip motion and the driving force.

Invoking the relation $\omega = \omega_0\sqrt{1 + C_i^{\rm eff}/C}$, the oscillation frequency can be expressed in terms of an effective force gradient[6, 7]

$$C_i^{\rm eff} = -\frac{2}{\pi a_1}\int_{-1}^{1} F_{\rm int}(z_0 + a_1 u)\frac{u}{\sqrt{1-u^2}}\,du \;+\; \frac{F_0\cos\Theta}{a_1}\,, \tag{2}$$

where we have used the substitution $\cos(\omega t) = u$. Note that the in-phase component of the driving force, $F_0 \cos\Theta$, acts as an additional spring constant, which in turn gives rise to an additional shift of the oscillation frequency.

A complementary relation that connects the driving force to the damping coefficient is obtained from an energy balance argument. In the steady state, the net work executed by the driving force in the course of one oscillation cycle must be equal to the energy dissipation due to the viscous interaction, yielding

$$F_0 \sin\Theta = \frac{2a_1\omega}{\pi}\int_{-1}^{1} \Gamma(z_0 + a_1 u)\sqrt{1-u^2}\,du\,. \tag{3}$$

The out-of-phase component of the driving force, $F_0 \sin\Theta$, is hence proportional to a velocity weighted average of the damping coefficient that is probed by the tip.

For an arbitrary phase angle $\Theta \neq \pm 90^\circ$ the dissipative interaction couples to the frequency shift via the $F_0 \cos\Theta$ term in Eq. (2). Thus the oscillator frequency is in general different from the eigenfrequency of the resonator[8]. In order to decouple the resonance frequency from the dissipative interaction a phase angle of $\Theta = \pm 90^\circ$ must be selected. This issue is crucial for quantitative dynamic force sensing. Henceforth we assume that driving force and resonator response are mutually 90° out of phase and we can thus unequivocally identify a frequency shift with conservative interactions and a driving force with dissipative interactions, respectively. Note that the phase angle corresponding to the proper operating point can deviate substantially from the nominal 90° value in a real experiment due to additional phase shifts in the apparatus. The proper operating point can be easily identified, however, as it coincides with a minimum of the driving force amplitude F_0 required to sustain a constant oscillation amplitude a_1.

As discussed in Refs. [7] and [9] the conservative interaction force law $F_{\rm int}(x)$ can be determined from a measurement of the effective force gradient $C_i^{\rm eff}(z_0)$ as a function of the offset

parameter z_0, termed force gradient curve, which involves the inversion of the integral operator Eq. (2). A similar methodology can be invoked for extracting the damping coefficient function $\Gamma(x)$ from a measurement of the driving force curve $F_0(z_0)$. To this end we rewrite Eq. (3) to express $u = x/a_1$ in terms of the physical tip-sample distance x

$$F_0(z_0) = \mathcal{A}(\Gamma) = \frac{2\omega}{\pi} \int\limits_{z_0-a_1}^{z_0+a_1} \Gamma(x) \sqrt{1 - \left(\frac{x-z_0}{a_1}\right)^2}\, dx\,. \tag{4}$$

The above convolution integral cannot be inverted in closed form. Very often, however, the range of interaction is short compared to the vibration amplitude. In this case, one can approximate the kernel by the leading square-root term at closest sample approach, $z = z_0 - a_1$, and one can extend the integration to infinity,

$$F_0(z) = \mathcal{B}(\Gamma) = \frac{2^{3/2}\omega}{a_1^{1/2}\pi} \int\limits_{z}^{\infty} \Gamma(x) \sqrt{x-z}\, dx\,. \tag{5}$$

Invoking Laplace transforms [10] one readily finds the inverse of the approximate operator $\mathcal{B}$

$$\Gamma(x) = \mathcal{B}^{-1}(F_0) = \frac{a_1^{1/2}}{2^{1/2}\omega} \int\limits_{x}^{\infty} \frac{\frac{d^2}{dz^2}F_0(z)}{\sqrt{z-x}}\, dz\,. \tag{6}$$

The damping coefficient obtained by means of the large amplitude inversion operator $\mathcal{B}^{-1}$ does not, in general, exactly reproduce the measured driving force curve upon substitution into Eq. (4). However, using the iterative scheme described in Ref. [9] the solution can be systematically improved until satisfactory consistency is obtained.

Inversion of Eq. (4) is trivial for exponentially decaying driving force curves, $F_0(z) = F_0 \exp(-\kappa z)$, which are eigenfunctions of the convolution operator $\mathcal{A}$:

$$\Gamma(x) = \frac{1}{\lambda} F_0 \exp(-\kappa x)\,, \tag{7}$$

where the eigenvalue is given by

$$\lambda = \frac{2\omega}{\pi} \int\limits_{0}^{2a_1} \exp(-\kappa y) \sqrt{1 - \left(\frac{y-a_1}{a_1}\right)^2}\, dy \overset{\kappa a_1 \to \infty}{=} \frac{2^{1/2}\omega}{(\pi a_1 \kappa^3)^{1/2}}\,. \tag{8}$$

For inverse power laws, $F_0(z) = F_0/z^p$, on the other hand, the damping coefficient decays more rapidly than the corresponding driving force curve because of the derivative operation in $\mathcal{B}^{-1}$. In the large amplitude limit, $a_1 \gg z$, one finds

$$\Gamma(x) = \frac{p(p+1)N_p a_1^{1/2}}{2^{1/2}\omega} \frac{F_0}{x^{p+3/2}}\,, \tag{9}$$

where $N_p = \int_0^\infty y^{-1/2}(1+y)^{-(p+2)} dy$ is a normalization constant of the order of one ($N_1 \simeq 1.132$, $N_2 \simeq 0.935$, $N_3 \simeq 0.813$, $N_4 \simeq 0.727$).

Very often, experimentally measured driving force curves cannot be represented by a simple exponential or power law. In such cases it is most convenient to recover the corresponding damping coefficient by means of direct inversion. For example, we consider interaction force

curves, see Fig. 2 of Ref. [3]. The data were measured on a Si(111) substrate using a Si cantilever tip. The conservative interaction force shown in Fig. 3(d) derived from the frequency shift curve Fig. 2(a) has been discussed previously[7]. The driving force curve $F_0(z)$, Fig. 3(a), is obtained from the power loss curve $P(z)$, Fig. 2(b), using the transformation $F_0 = 2P/(\omega a_1)$, where $\omega = 2\pi \times 153$ kHz is the oscillator frequency and $a_1 = 9.5$ nm is the oscillation amplitude (note that a constant offset of $P_0 = 6 \times 10^{-14}$ W, which accounts for the intrinsic damping of the force sensor, has been subtracted).

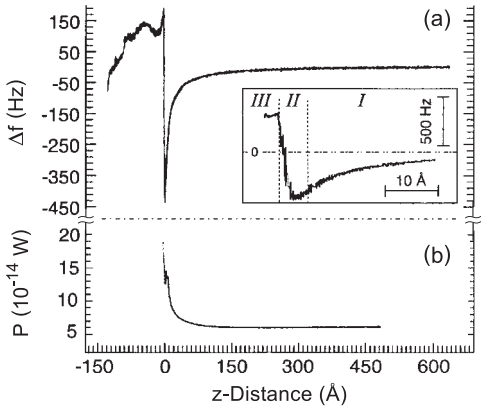

Figure 2: (a) Frequency shift and (b) power loss measured on a Si(111) substrate using a Si cantilever tip (adapted from Ref. [3], used with permission).

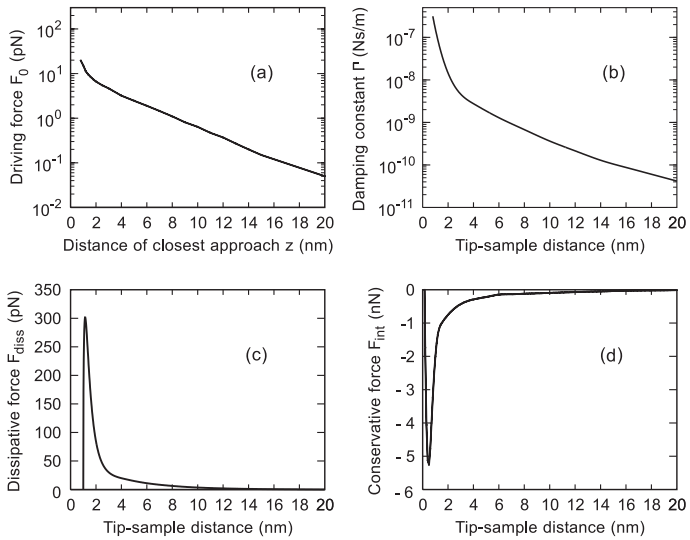

Figure 3: (a) Amplitude of the driving force versus distance of closest sample approach as derived from the power loss curve, Fig. 2(b). (b) Damping constant versus tip-sample distance corresponding to the driving force curve (a). (c) Dissipative force versus tip-sample distance as experienced by the tip in an oscillation approaching the sample by $z = 1$ nm at the closest point. (d) Conservative interaction force versus tip-sample distance as derived from the frequency shift curve Fig. 2(a).

The experimental power-loss curve shows irregularities in the range of the adhesion maximum $0 \leq z \leq 1$ nm, which indicates that some genuine irreversibilities associated with strong adhesive forces take place in this regime. As explained in the introduction, such hysteretic interactions cannot be represented by a viscous damping constant $\Gamma(x)$. Hence, we restrict our analysis to the regime $z \geq 1$ nm in which the power-loss curve is a continuously decaying smooth function. In fact, it follows from Eq. (6) that the damping coefficient is in essence proportional to the square root of a length scale, $\sqrt{(dF_0/dz)/(d^2F_0/dz^2)}$,[11] times the curvature of the driving force curve d^2F_0/dz^2 . Hence, the curvature must be a strictly positive number, otherwise unphysical negative values for the damping coefficient are obtained. This condition imposes, at least in the large amplitude limit, a stringent criterion that allows one to identify regimes in which the dissipative mechanism definitely cannot be described exclusively in terms of a viscous damping force.

The damping constant as a function of tip-sample distance was calculated using Eqs. (4) and (6) and the iterative scheme of Ref. [9]. Three iterations were sufficient to obtain overall consistency on the percent level, whereby all essential features were captured by the lowest-order approximate solution $\mathcal{B}^{-1}(F_0)$ on a ten-percent level already. The most prominent feature of the damping constant curve is the dramatic increase by almost two orders of magnitude in the tip-sample distance interval between 1 and 2 nm. Note that the driving force increases much less rapidly, namely only by a factor of 3, in this regime. The strong enhancement of the damping constant is due to the derivative operation in Eq. (6) and is thus a general phenomenon of the inversion.

Given the damping constant function $\Gamma(x)$ one can readily calculate the dissipative force that is acting on the tip during the oscillatory motion

$$F_{\rm diss}(z + a_1(u+1)) = \Gamma(z + a_1(u+1))\sqrt{1-u^2}\,, \tag{10}$$

where $-1 \leq u = \cos\omega t \leq 1$ denotes the orbital parameter. The dissipative force corresponding to $z = 1$ nm is shown in Fig. 3(c). Consistent with the sharp increase of the damping constant at short tip-sample distance, the dissipative force peaks at close sample proximity. The peak amplitude of 300 pN is one order of magnitude larger than the corresponding average driving force. It thus looks as if the tip hits against a viscous wall. Nevertheless, the adhesive force, which is of the order of 2.5 nN at $z = 1$ nm (see Fig. 3(d)), still dominates the overall tip-sample interaction. Moreover, inspection of the force curve in Fig. 3(d) suggests that the tip apex is still several tenths of a nanometer away from the sample surface at this point. Thus, the dissipation must be induced by long-range interactions.

Electrical dissipation due to tip-induced motion of space charges provides a likely explanation for the damping. In particular it has been argued that in semiconductors, damping constants of the order of $10^{-9}...10^{-8}$ Nsm^{-1} are to be expected in a typical atomic force microscopy geometry with samples having a resistivity of the order of 0.1 Ωm[12]. Alternatively, it has recently been shown that a damping coefficient can be associated with fluctuating random charges and currents which are responsible for the Van der Waals interaction[13]. The theory predicts that the damping coefficient is proportional to $1/x^4$ for good conductors. Indeed, the extracted damping coefficient follows an inverse power law at short distances with an exponent of the order of 3 to 4. However, as sample and tip are semiconductors, the situation is substantially more complex than for metallic bodies, viz. surface states and band bending give rise to space charge effects, which must be taken into account as well. Nevertheless, the use of refined analysis methods as described in this Letter provides detailed information on

the interaction mechanisms which, in turn, will form the basis for comprehensive theoretical investigations in the future.

It is a pleasure to acknowledge stimulating discussions with Graham Cross, Franz Giessibl, and Peter Blöchl.

References

[1] F. Giessibl, Science **267**, 68 (1995).

[2] Y. Sugawara, M. Ohta, H. Ueyma, S. Morita, F. Osaka, S. Ohkouchi, M. Suzuki, and S. Mishima, J. Vac. Sci. Technol. B **14**, 953 (1996).

[3] R. Lüthi, E. Meyer, M. Bammerlin, A. Baratoff, L. Howald, Ch. Gerber, and H.J. Güntherodt, Surface Rev. Lett. **4**, 1025 (1997).

[4] For a discussion of examples, see e.g. U. Dürig, Surf. Interface Anal. **27**, 467 (1999).

[5] U. Dürig, accepted for publication New J. of Phys. (2000).

[6] F. J. Giessibl, Phys. Rev. B **56**, 16010 (1997).

[7] U. Dürig, Appl. Phys. Lett. **75**, 433 (1999).

[8] U. Dürig, H.R. Steinauer, and N. Blanc, J. Appl. Phys. **82**, 3641 (1997).

[9] U. Dürig, Appl. Phys. Lett. **76**, 1203 (2000).

[10] See e.g. Gustav Doetsch, *Handbuch der Laplace-Transformation*, Band III, chapter 25, (Birkhäuser Verlag, Basel, 1956) p. 157 ff; note that $\Gamma(x) = d^2/dx^2\Phi(x)$ is written as the second derivative of some function Φ, which can be written as a product of well-defined Laplace transforms of the driving force function $F_0(z)$ and of a kernel $1/\sqrt{x}$

[11] F.J. Giessibl and H. Bielefeldt, Phys. Rev. B (to appear March 15, 2000).

[12] W. Denk and D.W. Pohl, Appl. Phys. Lett. **59**, 2171 (1991).

[13] I. Dorofeyev, H. Fuchs, G. Wenning, and B. Gotsmann, Phys. Rev. Lett. **83**, 2402 (1999).